Amiodarone Alters Late Endosomes and Inhibits SARS Coronavirus Infection at a Post-Endosomal Level

Konrad Stadler[1*], Huy Riem Ha[2], Vincenzo Ciminale[3], Carlo Spirli[4‡], Giulietta Saletti[1], Marco Schiavon[5], Daniela Bruttomesso[6], Laurent Bigler[7], Ferenc Follath[2], Andrea Pettenazzo[8], and Aldo Baritussio[9]

[1]Novartis Vaccines, Siena, Italy; [2]Cardiovascular Therapy Research Laboratory, Department of Internal Medicine, University Hospital of Zurich, Zurich, Switzerland; [7]Institute of Organic Chemistry, University of Zurich, Zurich, Switzerland; [4]Venetian Institute of Molecular Medicine, University of Padova, Padova, Italy; [5]Divisione di Chirurgia Toracica, and Departments of [3]Oncological and Surgical Sciences, [6]Clinical Medicine, [8]Pediatrics, and [9]Medical and Surgical Sciences, University of Padova, Padova, Italy

Amiodarone interferes with the endocytic pathway, inhibits proteolysis, and causes the formation of vacuoles, but uptake and intracellular distribution of the drug, origin of vacuoles, and functional consequences of amiodarone accumulation remain unclear. Our objective was to study amiodarone uptake, clarify the origin of vacuoles, and investigate the effect of amiodarone on the life cycle of the coronavirus responsible for the Severe Acute Respiratory Syndrome (SARS), which, to enter cells, relies on the proteolytic cleavage of a viral spike protein by the endosomal proteinase cathepsin L. Using alveolar macrophages, we studied uptake of ^{125}I-amiodarone and ^{125}I-B2, an analog lacking the lateral group diethylamino-β-ethoxy, and analyzed the effects of amiodarone on the distribution of endosomal markers and on the uptake of an acidotropic dye. Furthermore, using Vero cells, we tested the impact of amiodarone on the *in vitro* spreading of the SARS coronavirus. We found that (*1*) amiodarone associates with different cell membranes and accumulates in acidic organelles; (*2*) the diethylamino-β-ethoxy group is an important determinant of uptake; (*3*) vacuoles forming upon exposure to amiodarone are enlarged late endosomes; (*4*) amiodarone inhibits the spreading *in vitro* of SARS coronavirus; and (*5*) trypsin cleavage of the viral spike protein before infection, which permits virus entry through the plasma membrane, does not impair amiodarone antiviral activity. We conclude that amiodarone alters late compartments of the endocytic pathway and inhibits SARS coronavirus infection by acting after the transit of the virus through endosomes.

Keywords: amiodarone; endocytic pathway; SARS coronavirus

Amiodarone, an antiarrhythmic agent used to treat supraventricular and ventricular arrhythmias, has peculiar pharmacokinetics. After intestinal absorption or intravenous administration, it leaves the serum compartment with a half-life of 10 to 20 hours and accumulates extensively in peripheral tissues (1). Two characteristics seem important in determining its distribution through the body: the extreme hydrophobicity, which may explain the preferential accumulation into structures rich of lipids, and the presence of a diethylamino-β-ethoxy group, which may favor the association with acidic organelles (2–4). In fact, amiodarone inhibits the degradation of surfactant protein A (SP-A) (a calcium-dependent lectin taken up by alveolar macrophages and degraded into lysosomes) (4); decreases the size of the lysosomal compartment (4); and causes the accumulation of lyso-bis-phosphatidic acid, a rare phospholipid associated with the internal vesicles of late endosomes/multivesicular bodies (2, 5). On the basis of these findings, it has been suggested that amiodarone may affect late compartments of the endocytic pathway, but the mechanism of uptake of the drug, its cellular distribution, and the role played by the diethylamino-β-ethoxy group remain unclear.

A peculiar consequence of amiodarone administration is the formation of vacuoles, multilamellar inclusion bodies and crystalline-like deposits in different cell types; however, the origin of these structures is also unknown (3, 6).

To clarify some of these points, using alveolar macrophages, we analyzed uptake and intracellular distribution of ^{125}I-amiodarone and ^{125}I-B2, an analog lacking the diethylamino-β-ethoxy group (7). Furthermore, using confocal microscopy, we analyzed the effects of amiodarone on the distribution of markers of early and late endosomes and on the uptake of an acidotropic dye. Finally, since infection of target cells by the coronavirus (CoV) responsible of the Severe Acute Respiratory Syndrome (SARS) relies on the endosomal cleavage of a viral surface protein, we also studied the impact of amiodarone on the *in vitro* spreading of this newly emergent infectious agent (8).

SARS-CoV is an enveloped virus, with a positive-stranded RNA genome, presenting club-shaped protrusions made by trimers of the spike (S) protein. The first step in the viral life-cycle is the binding of the S protein to its receptor, the angiotensin-converting enzyme 2 (ACE2). Subsequently the virus is taken up by receptor-mediated endocytosis, ending into an acidic endosomal compartment where the S protein is proteolitically cleaved by the endosomal protease cathepsin L. Protein S then triggers the mixing of viral and endosomal membranes, causing the release of the viral genome into the cytoplasm (9–16). Having found that amiodarone perturbs late compartments of the endocytic pathway, we tested its impact on the life-cycle of the SARS-CoV.

CLINICAL RELEVANCE

This article shows that vacuoles are enlarged late endosomes and that amiodarone inhibits *in vitro* severe acute respiratory syndrome coronavirus infection acting after the delivery of the viral genome into the cytoplasm.

MATERIALS AND METHODS

Materials

Antibodies were from Stressgen Biotechnologies, Eugene, OR (Rab4 and Fas); Ancell, Bayport, MN (CD63), Abcam, Cambridge, UK (EEA1); and Athens Research and Technology, Athens, CA (cathepsin L).

(*Received in original form June 12, 2007 and in final form November 17, 2007*)

*Present affiliation: International Vaccine Institute, Seoul, Korea.

‡Present affiliation: Department of Internal Medicine, Section of Digestive Diseases, Yale University, New Haven, Connecticut.

This work was supported in part by Fondi ex 60% to A.B. and by a generous gift from Mr. Antonio Fiore.

Correspondence and requests for reprints should be addressed to Aldo Baritussio, M.D., Clinica Medica I, Department of Medical and Surgical Sciences, University of Padova, 35128 Padova, Italy. E-mail aldo.baritussio@unipd.it

Am J Respir Cell Mol Biol Vol 39. pp 142–149, 2008
Originally Published in Press as DOI: 10.1165/rcmb.2007-0217OC on February 28, 2008
Internet address: www.atsjournals.org

Amiodarone was from Sigma (St. Louis, MO). B2 (2-butyl-3-(3′,5′-diiodo-4-hydroxy)-benzofuran) was synthesized as reported (7).

^{125}I-amiodarone (specific activity 34.7 Ci/mmol) and ^{125}I-B2 (3.36 Ci/mmol) were prepared following the method of Bellen and coworkers (17).

Water solubility and interaction with membranes of amiodarone and B2 were measured as reported (18, 19).

Vero cells (ATCC CCL-81) were maintained in GlutaMAX I (Gibco, Carlsbad, CA), 1% penicillin-streptomycin, 5% heat-inactivated fetal bovine serum (HyClone, Logan, UT). Alveolar macrophages, obtained after institutional approval and written consent from lung lobes resected for lung cancer, were maintained in Ringer Buffered 0.1% Albumin (RBA) (4).

Binding/Uptake of ^{125}I-Amiodarone and ^{125}I-B2

Macrophages, exposed for 60 minutes to medium or to 2.0 μM phenylarsine oxide, 2.5 mM amantadine hydrochloride, 1.5 μM filipin, 10 μM cytochalasin D, 0.1 μM wortmannin, 0.1 μM bafilomycin A_1, or 0.1 μM concanamycin A (all from Sigma), were incubated for 0 to 90 minutes with 0.2 μM ^{125}I-amiodarone or ^{125}I-B2 before measuring cell radioactivity. In some experiments fractions of the postnuclear supernatant (4, 20) were tested for radioactivity, protein (21), arylsulfatase (22), Rab4, CD63, and Fas (by Western blotting).

Immunofluorescence

Macrophages exposed to 0 to 10 μM amiodarone for 24 hours were fixed, permeabilized, incubated with anti-EEA1 and anti-CD63 antibodies, exposed to alexa 488– or alexa 546–conjugated secondary antibodies (Molecular Probes Europe BV, Leiden, The Netherlands), and analyzed by laser scanning confocal microscopy (Zeiss LSM510; Zeiss, Milan, Italy) (23).

Uptake of Lysosensor

Macrophages, incubated with 0 to 10 μM amiodarone for 24 hours, were exposed for 30 minutes to 1 μmol/L LysoSensor Green DND-189 (Molecular Probes) (24). Confocal images were then obtained (Nikon Eclipse TE300; Nikon, Tokyo, Japan), and emitted fluorescence was measured (Till Photonics, Martinsried, Germany).

Effect on Cathepsin L

Macrophages were exposed for 24 hours to 0 or 10 μM amiodarone, before analyzing cathepsin L in cell lysates by Western blotting (25).

Effects of Amiodarone on SARS-CoV Infection

Vero cell monolayers in 24-well tissue culture plates, pretreated with 0 to 50 μM amiodarone for 2 hours, were infected with SARS-CoV at a multiplicity of infection (m.o.i.) of 1 for 1 hour at 37°C. Cells were then washed with PBS and incubated over night in the presence of amiodarone. Virus released in the supernatant was titrated on Vero cells and $TCID_{50}$ calculated according to Spaerman-Kaerber.

Trypsin Treatment

Vero cells were treated for 1 hour at 37°C with medium, 40 mM NH_4Cl, or with amiodarone (10 or 50 μM). SARS-CoV was then added for 1 hour at 4°C (m.o.i. of 1). After removal of the inoculum, cells were washed twice with MEM without FCS before being treated for 5 minutes at room temperature with L-1-tosylamido-2-phenylethyl chloromethyl ketone-treated trypsin (10 μg/ml; Sigma). After trypsin removal cells were incubated over night in growth medium, NH_4Cl, or amiodarone, and viral titers in the supernatant were determined (13–15).

Statistical Analysis

Data are means ± SEM or means ± 95% confidence interval (CI). Differences were analyzed with paired *t* test, Dunnet's test, or Dunn's test. $P < 0.05$ was deemed significant.

RESULTS

Physicochemical Properties of Amiodarone and B2

Amiodarone was more water-soluble than B2, especially at acidic pH. In fact, as the pH was lowered from 7.4 to 5.0 the solubility in water of amiodarone increased from 0.069 ± 0.005 to 2.04 ± 0.11 μM, while that of B2 increased from 0.009 ± 0.0001 to 0.10 ± 0.01 μM (differences between amiodarone and B2 and between pH5.0 and 7.4 all statistically significant). The affinity of amiodarone for membranes, expressed as $\log k_{IAM}$, was significantly greater than that of B2 at pH 7.4 (respectively 4.23 ± 0.02 versus 3.20 ± 0.04), but smaller than that of B2 at pH 5.0 (3.63 ± 0.04 versus 4.57 ± 0.08).

Recently Bergstrom and coworkers reported that the solubility in water of amiodarone increases by 5 orders of magnitude as the pH is lowered from 7.4 to 5.0 (18). The reason for the discrepancy with our findings is unclear. It could be due to the fact that we started with 4 μM amiodarone in methanol (the highest concentration possible), while Bergstrom and colleagues started with an excess of solid drug.

Binding/Uptake of Amiodarone and B2 by Alveolar Macrophages

Except for confocal microscopy, all studies on human alveolar macrophages presented in this work have been previously done on rabbit alveolar macrophages. We found no difference between species considering the following: (*1*) ^{125}I-amiodarone uptake and distribution among organelles of the postnuclear supernatant; (*2*) effects of amiodarone on cell morphology at the EM level; (*3*) effect of amiodarone on the uptake of Lysosensor; (*4*) effect of amiodarone on cell viability. Thus we are reasonably sure that the effects seen on human alveolar macrophages were not related to their origin from resected lungs arboring neoplasia in sections different from those subjected to bronchoalveolar lavage.

As shown in Figure 1A, amiodarone associated rapidly with alveolar macrophages. Binding/uptake was linear over time and was critically dependent upon the presence of the diethylamino-β-ethoxy group, since ^{125}I-B2, which lacks this group, associated with macrophages 50 times more slowly than amiodarone (Figure 1).

Clathrin-mediated endocytosis, caveolae, the vectorial transfer of materials through the endocytic pathway, fluid phase endocytosis, or the cytoskeleton can be inhibited or perturbed without change in the net uptake of amiodarone. In fact, phenylarsine oxide and amantadine (inhibitors of clathrin-mediated endocytosis), filipin (inhibitor of endocytosis through caveolae), cytochalasin D (a disassembler of the cytoskeleton), and wortmannin (which inhibits fluid phase endocytosis, phagocytosis, and the vectorial movement of materials through the endocytic pathway) did not influence the association of ^{125}I-amiodarone with macrophages (Figure 1B). On the other side, bafilomycin A_1 and concanamycin A, which dissipate vacuolar acidity by inhibiting V-ATPase, decreased uptake without abolishing it (Figure 1B). Since the inhibitors used had no detrimental effect on cell viability, these results suggest that there is no preferential mechanism of uptake of amiodarone and that amiodarone, besides accumulating into acidic organelles, associates also with other cell structures. In fact, in a series of experiments in which we incubated macrophages with ^{125}I-amiodarone for 0, 30, 60, and 120 minutes and then subjected the postnuclear supernatant to a series of differential centrifugations each lasting 10 minutes ($3{,}000 \times g$, $6{,}000 \times g$, $10{,}000 \times g$, $20{,}000 \times g$, $100{,}000 \times g$), amiodarone accumulated in all pellets. Most of the radioactivity (over 85% of total) was associated with the $3{,}000 \times g$, $6{,}000 \times g$, and $10{,}000 \times g$ pellets, while the $100{,}000 \times g$ supernatant contained at any time less than 2% of total radioactivity (not shown), indicating that free iodine represented a minor fraction of total radioactivity.

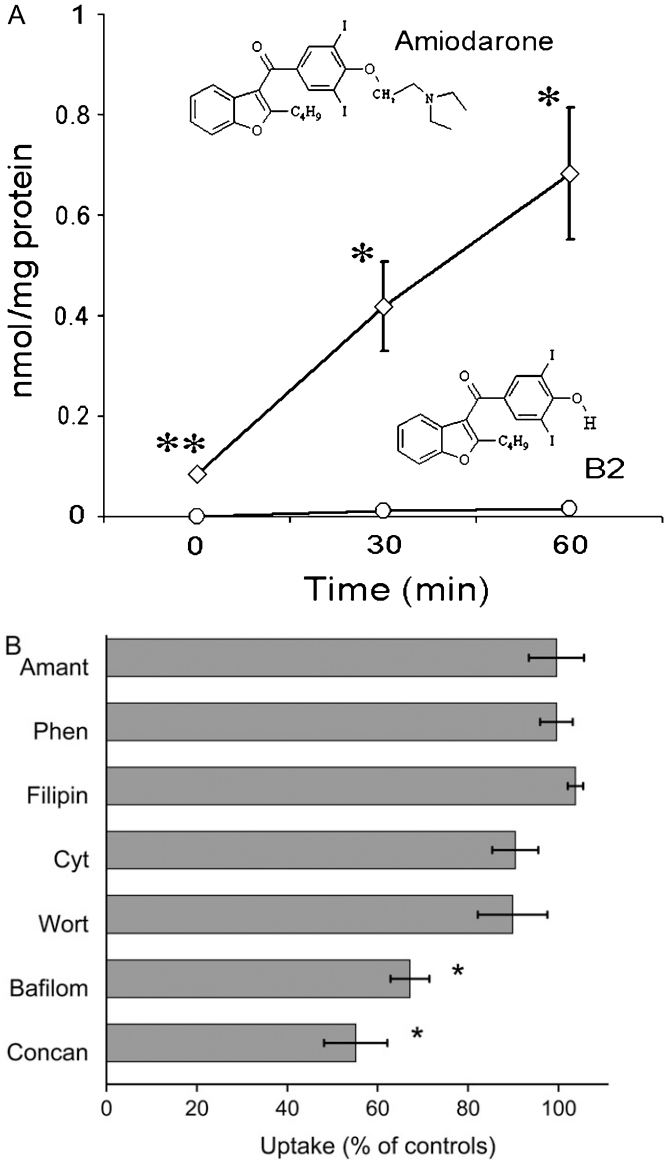

Figure 1. Binding/uptake of ^{125}I-amiodarone and ^{125}I-B2 by human alveolar macrophages. (*A*) Adhering cells (10^6) were incubated with 0.2 μM ^{125}I-amiodarone or ^{125}I-B2 and cell associated radioactivity was measured at the indicated times. M ± SE, $n = 4$. Different from B2: *$P < 0.03$, **$P < 0.01$ (paired t test). (*B*) Effect of inhibitors on binding/uptake of amiodarone by alveolar macrophages. Cells exposed for 60 minutes to plain medium (controls) or to 2.5 mM amantadine hydrochloride (Amant), 2.0 μM phenylarsine oxide (Phen), 1.5 μM filipin, 10 μM cytochalasin D (Cyt), 0.1 μM wortmannin (Wort), 0.1 μM bafilomycin A_1 (Bafilom), or 0.1 μM concanamycin A (Concan), were incubated for 60 minutes with 0.2 μM ^{125}I-amiodarone before measuring cell-associated radioactivity ($n = 3$–6). Uptake from control cells = 100%. *Different from all other except bafilomycin or concanamycin, $P < 0.05$ by ANOVA.

Distribution of Amiodarone among Organelles of the Postnuclear Supernatant

To clarify the fate of amiodarone after uptake, we incubated alveolar macrophages with 0.2 μM ^{125}I-amiodarone and then followed the distribution of radioactivity among organelles isolated from the post nuclear supernatant. In the system we used the lysosomes migrate toward the bottom of the tube, early and late endosomes remain in the upper third, fragments of the plasma membrane remain at the top and mitochondria collect to the very bottom of the gradient, as deduced from the distribution of specific markers: arylsulfatase (lysosomes), Rab4 (early endosomes), CD63 (late endosomes), Fas (plasma membrane) (Figure 2) (23). Cytochrome C oxydase (marker of mitochondria) concentrates in fractions 1–4, while EEA1 (another marker of early endosomes) has same distribution of Rab4 (not shown).

As shown in Figure 2, when macrophages were incubated with 0.2 μM ^{125}I-amiodarone, the radioactivity gradually accumulated into organelles migrating at the extremes of the gradient, collecting to a greater extent toward the bottom. Treatment with bafilomycin decreased markedly the radioactivity associated with both populations of organelles (Figure 2). Thus it appears that amiodarone, presented to cells at low concentrations, associates in a time-dependent manner with diverse organelles of the postnuclear supernatant, some of which can be identified as endosomes and lysosomes on the basis of sedimentability, distribution of markers, and sensitivity to treatment with bafilomycin A1.

These results were obtained from macrophages incubated with 0.2 μM amiodarone, while patients are chronically exposed to concentrations ranging from 1 to 4 μM. To test the effect of higher concentrations of amiodarone, we incubated alveolar macrophages for 16 hours both with 0.2 and with 10.0 μM ^{125}I-amiodarone, and then analyzed the distribution of radioactivity among organelles of the postnuclear supernatant. As shown in Figure 3, the concentration of amiodarone had marked effects on the distribution of radioactivity. In fact, when present at low concentration, amiodarone distributed mostly toward the bottom of the gradient, suggesting a preferential accumulation into lysosomes. At high concentrations amiodarone accumulated mostly toward the top of the gradient, suggesting a preferential accumulation into endosomes.

^{125}I-B2 was taken up by alveolar macrophages to such a low extent that the radioactivity of the postnuclear supernatant was barely greater than background (not shown).

Vesicles Forming upon Exposure to Amiodarone

To characterize the vesicles forming upon exposure to amiodarone, we analyzed the effects of the drug on the distribution of markers commonly used to identify early and late endosomes, respectively EEA1 and CD63. As shown in Figure 4, in control cells EEA1 decorated a population of round organelles, mainly located at one extreme of the cell, while CD63 was associated with structures presenting both as puncta and as a tenuous net scattered throughout the cytoplasm, a pattern compatible with the known tubulo-vesicular morphology exhibited by late endosomes in macrophages (26). Few organelles were positive for both markers (Figure 4). Amiodarone did not influence the distribution of EEA1, but changed dramatically the distribution of CD63, which was mostly located at the rim of large vacuoles placed at the cell periphery (Figure 4). As in control cells, very few organelles were positive for both markers. Thus amiodarone does not perturb appearance and distribution of early endosomes, but has marked effects on the organization of late endosomes.

Effect of Amiodarone on the Uptake of Lysosensor DND-189

Amiodarone changes dramatically the distribution of Lysosensor Green DND-189, an acidotropic dye that accumulates into acidic organelles as the result of protonation and whose fluorescence intensity is proportional to acidity (24). In fact, control macrophages accumulated Lysosensor as small vesicles clustered near the nucleus and also displayed a diffuse staining of the cytoplasm, while macrophages treated with 10 μM

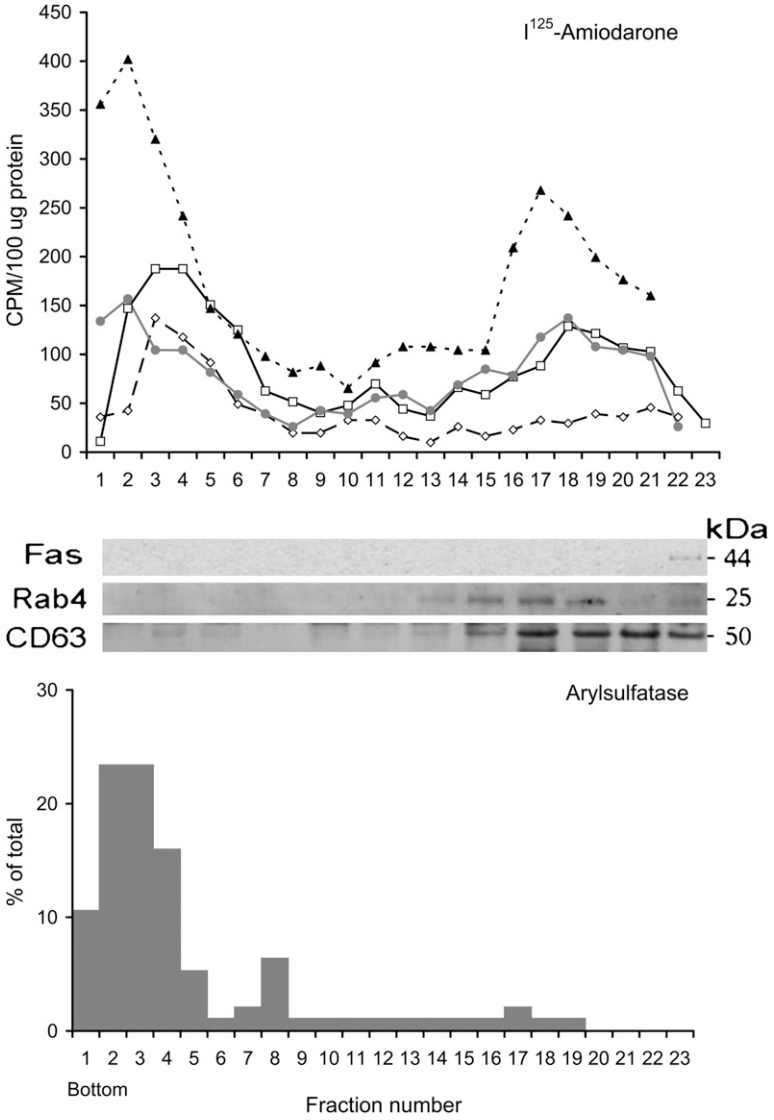

Figure 2. Association of amiodarone with organelles of the postnuclear supernatant. Adhering human alveolar macrophages (5×10^6cells) were exposed to 0.2 μM ^{125}I-amiodarone ± 0.5 μM bafilomycin A_1 for the indicated times. The postnuclear supernatant was then fractionated by density gradient centrifugation and on fractions radioactivity was counted (*top*); the presence of Fas, Rab 4, and CD63 was analyzed by Western blotting (*middle*); and arylsulfatase activity was measured (*bottom*). The figure is representative of three experiments. *Diamonds*, 30 minutes; *squares*, 60 minutes; *triangles*, 120 minutes; *circles*, 120 minutes + Bafilomycin.

amiodarone accumulated Lysosensor in large vacuoles located mostly at the cell periphery (Figure 5A). Besides changing the distribution of Lysosensor DND-189, amiodarone decreased the net uptake of the probe, as indicated by the decrease of fluorescence emitted by whole cells (Figure 5B). The effect was dose dependent and significant at 2 μM amiodarone. The lower uptake of Lysosensor in the presence of amiodarone appears to have been due to decreased uptake rather than to increased release of the probe, since cells loaded with Lysosensor and then exposed to amiodarone lost their fluorescence more slowly than cells loaded with Lysosensor and then exposed to plain medium (not shown).

Effect of Amiodarone on Cathepsin L

As shown in Figure 6, 10 μM amiodarone, did not change the total amount of catehepsin L present in lysates obtained from alveolar macrophages and did not affect the maturation of this enzyme, since the ratio between the immature procathepsin L (38 kD), the intermediate 30-kD form and mature cathepsin L (24, 25 kD) remained unchanged (25).

Effect of Amiodarone on SARS-CoV Infectivity

It has previously been shown that amiodarone inhibits the degradation of surfactant protein A, resulting in the accumulation of the uncleaved protein in an endosomal compartment (4). Since infection of target cells by the SARS-CoV is reliant on the proteolytic cleavage of the S protein by the lysosomal cysteine proteinase cathepsin L (13, 14), we explored the possibility of an effect of amiodarone on the life-cycle of the SARS-CoV. All work with live SARS-CoV was done in a biosafety level 3 facility at Novartis Vaccines, Siena, Italy. Preliminary experiments showed that amiodarone is taken up by Vero cells, the uptake being comparable with that of alveolar macrophages considering kinetics and sensitivity to inhibitors.

Vero cells were incubated for 2 hours with 0 to 50 μM amiodarone and then were infected with SARS-CoV (m.o.i. of 1). One hour after infection the cells were washed and further incubated in growth medium in the presence of the drug. The next day the cell culture supernatant was harvested and the virus was quantified by titration. As shown in Figure 7A, which presents the results of four independent experiments, amiodarone affected the life-cycle of SARS-CoV in a concentration-dependent manner: 5 μM amiodarone induced a significant diminution of the virus titer; 10 μM amiodarone decreased the virus titer 10 times; 50 μM amiodarone brought the virus titer below the detection limit, which was 10 $TCID_{50}$/ml in this assay.

Amiodarone can be toxic to cells (4, 7) and its antiviral activity could be due to decreased cell viability. To rule this out,

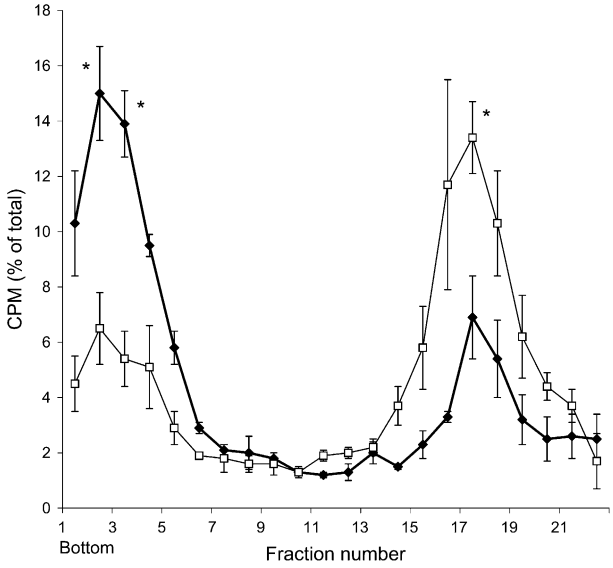

Figure 3. Effect of different amiodarone concentrations on the distribution of the drug among organelles of the postnuclear supernatant. Adhering human alveolar macrophages (5×10^6) were incubated with 0.2 (*diamonds*) or 10.2 (*squares*) μM ^{125}I-amiodarone for 16 hours. The postnuclear supernatant was then fractionated by density gradient centrifugation as reported in Figure 2, and the distribution of radioactivity through the gradient was analyzed. M ± SE ($n = 3$). Different from control, $*P < 0.02$ (paired *t* test).

Vero cells were incubated for 24 hours with 0 to 50 μM amiodarone and then their ability to incorporate propidium iodide was analyzed using a FACSCalibur (Becton Dickinson, San Jose, CA). We found that cell viability was greater than 97% up to 30 μM amiodarone, 91% at 40 μM amiodarone, and 83% at 50 μM amiodarone. Thus amiodarone has antiviral activity at concentrations at which it has no effect on viability.

The antiviral effect of amiodarone could be due to a direct effect of the drug on the SARS-CoV. To clarify this point, SARS-CoV in growth medium was incubated at 37°C for 24 hours without or with 10 μM amiodarone. Before titration on Vero cells, the two admixtures were diluted 10 times, so that the amiodarone concentration decreased to 1 μM (which has no effect on the propagation of SARS-CoV). We found no significant difference in virus titer between the two deposits (data not shown). In a further experiment SARS-CoV was incubated at 37°C for 24 hours with 5 or 50 μM amiodarone. Then the 50-μM amiodarone-virus admixture was diluted with fresh medium to 5 μM and both admixtures were titrated on Vero cells. We found no significant difference in virus titer between the two deposits (data not shown). We conclude, therefore, that a direct interaction of amiodarone with the SARS-CoV is unlikely or not significant.

SARS-CoV enters into target cells by binding through the S protein to the surface receptor ACE2. The virus is then taken up, ending in an acidic endosomal compartment where, after proteolysis by cathepsin L, protein S triggers the release of the viral genome into the cytoplasm. A mildly acidic pH environment in the endosome seems to be important, since infection can be blocked by lysosomotropic agents like NH_4Cl or chloroquine (13). In principle amidarone could decrease the infectivity of SARS-CoV by decreasing the density of surface receptors, by interfering with organelle acidification or by interfering with synthesis, maturation, or activity of cathepsin L. These mechanisms, however, are unlikely. In fact, amiodarone does not modify the density of ACE2 receptors on the cell surface, as determined by flow-cytometry using a human monoclonal antibody against ACE2 (not shown); does not inhibit organelle acidification (Ref. 4 and Figure 5); and does not interfere with synthesis and maturation of cathepsin L (Figure 6).

In a final experiment we tested whether amiodarone interferes with early stages of the virus life cycle, in particular those involving the endosomes, where the drug appears to be active. We reasoned that if the endosomes were the only site of interefence of amiodarone with the virus life cycle, then it could be possible to restore virus infectivity by trypsin treatment of SARS-CoV bound to target cells (which enables the virus to fuse directly with the plasma membrane and to infect cells without using the endosomal pathway). Accordingly, Vero cells were pre-incubated with amiodarone and then the virus was allowed to bind to the cells at 4°C. Afterward trypsin was added, to allow the fusion of virus and cell membranes and the direct release of the virus genome into the cytosol (15). Thereafter, cells were incubated in growth medium overnight and virus titer was determined. As shown in Figure 7B, trypsin

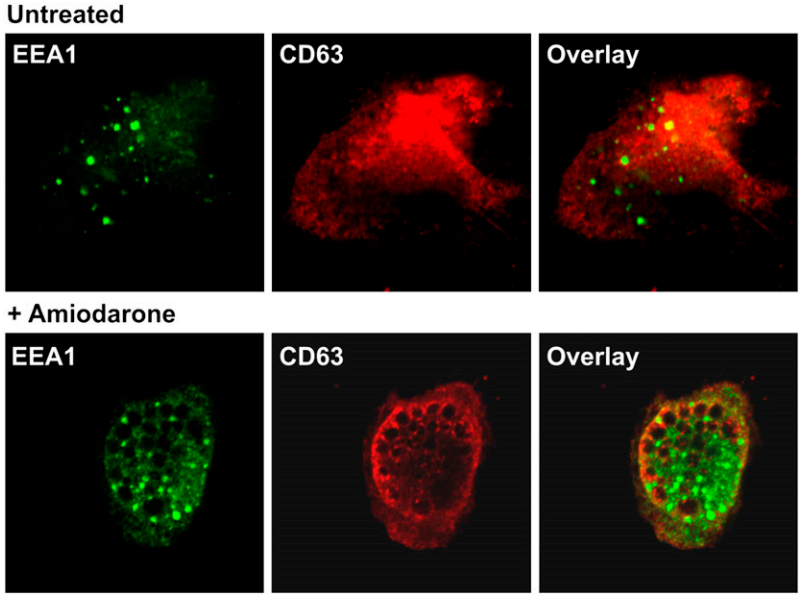

Figure 4. Vacuoles induced by amiodarone are enlarged late endosomes. Human alveolar macrophages were incubated for 16 hours with plain medium (controls) or with 10 μM amiodarone. Cells were then permeabilized and stained by indirect immunofluorescence using antibodies anti EEA1 as an early endosomal marker and antibodies anti CD63 as a late endosomal marker. Confocal images are shown with EEA1 appearing *green* and CD63 appearing *red*. Colocalized structures appear *yellow* in the merged image.

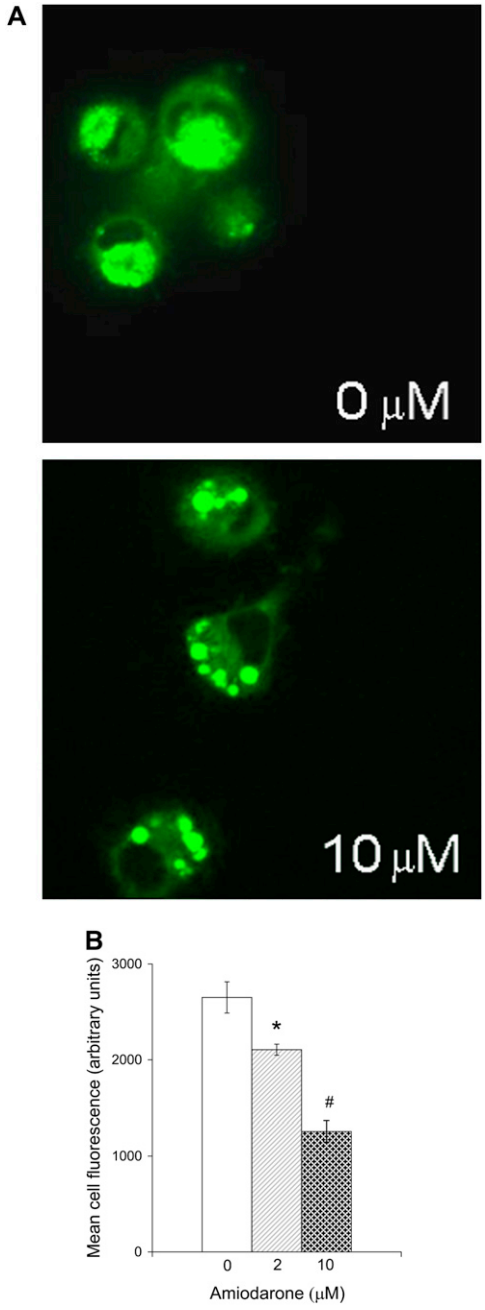

Figure 5. Effect of amiodarone on uptake and distribution of Lysosensor Green DND-189 by alveolar macrophages. Cells (10^6) incubated for 16 hours with medium (controls) or amiodarone at the indicated concentrations were exposed for 30 minutes to 1 μmol/L LysoSensor Green DND-189. After washing, confocal images were obtained (*A*) and the fluorescence emitted by individual cells at 505 nm in response to an excitation light of 440 nm was measured (*B*). Data are representative of three independent experiments in which the fluorescence emitted by 20 cells was measured. *Different from control, $P < 0.05$; #different from control and 2 μM amiodarone, $P < 0.01$ by ANOVA.

treatment of cell-bound virus could overcome the infection block mediated by ammonium chloride, the control in this experiment, but not the block induced by amiodarone, strongly indicating that amiodarone interferes with the SARS-CoV life cycle after delivery of the viral genome in the cytosol.

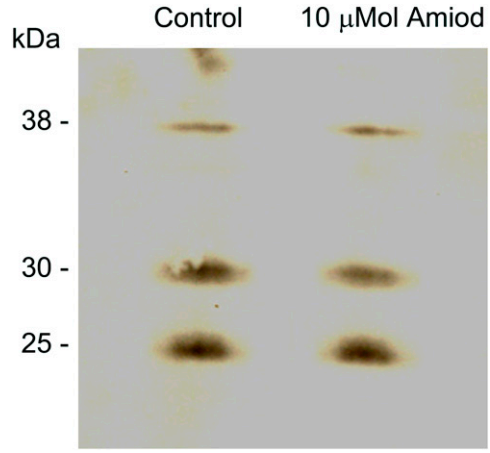

Figure 6. Amiodarone does not affect the total cell content or the maturation of cathepsin L. Alveolar macrophages (2×10^6 cells) were incubated for 24 hours with medium (controls) or with 10 μM amiodarone. Cell lysates (20 μg protein) were then fractionated by polyacrylamide gel electrophoresis, transferred on nitrocellulose, and probed with an antiserum anti–cathepsin L. *Bands* are pro–cathepsin L (38 kD), an intermediate form (30 kD) and mature cathepsin L (two bands of 24 and 25 kD not resolved under the conditions used). Representative of four experiments.

DISCUSSION

Binding/Uptake and Distribution of Amiodarone

Association of amiodarone with cells is greatly influenced by the lateral group diethylamino-β-ethoxy. In fact, at pH 7.4 amiodarone had greater solubility in water and higher affinity for membranes than B2, while at pH 5.0 amiodarone had greater solubility in water but lower affinity for membranes than B2, indicating that the diethylamino-β-ethoxy group may favor both the transfer of the drug from carrier proteins to the plasma membrane and accumulation into acidic organelles. It is clear, however, that association with acidic organelles is just one of the ways in which amiodarone accumulates inside cells, since the dissipation of vacuolar acidity decreases but does not abolish uptake.

From the present evidence, we propose that amiodarone could associate with the plasma membrane and then distribute to different cell compartments according to the section of the plasma membrane in which it happens to be. Amiodarone ending into early endosomes will follow the fate of these organelles along the endocytic pathway and, as the lumenal pH drops, it could move from the limiting membrane to the lumen. This interpretation can explain the distribution of the drug to all cell membranes, the lack of a preferential mechanism of uptake, the association with acidic organelles, the decreased uptake after dissipation of the vacuolar acidity, and the preferential association with lysosomes (which have the lowest internal pH).

Effects of Pharmacologic Concentrations of Amiodarone

Patients treated chronically with amiodarone have plasma concentrations ranging from 1 to 4 μM (1). We tried to reproduce this condition by exposing acutely alveolar macrophages to 10 μM amiodarone, a treatment that does not affect viability and induces the formation of vacuoles similar to those seen *in vivo* (4, 7). We now show that the vacuoles are enlarged late endosomes and that early endosomes maintain their usual configuration, in agreement with previous evidence indicating

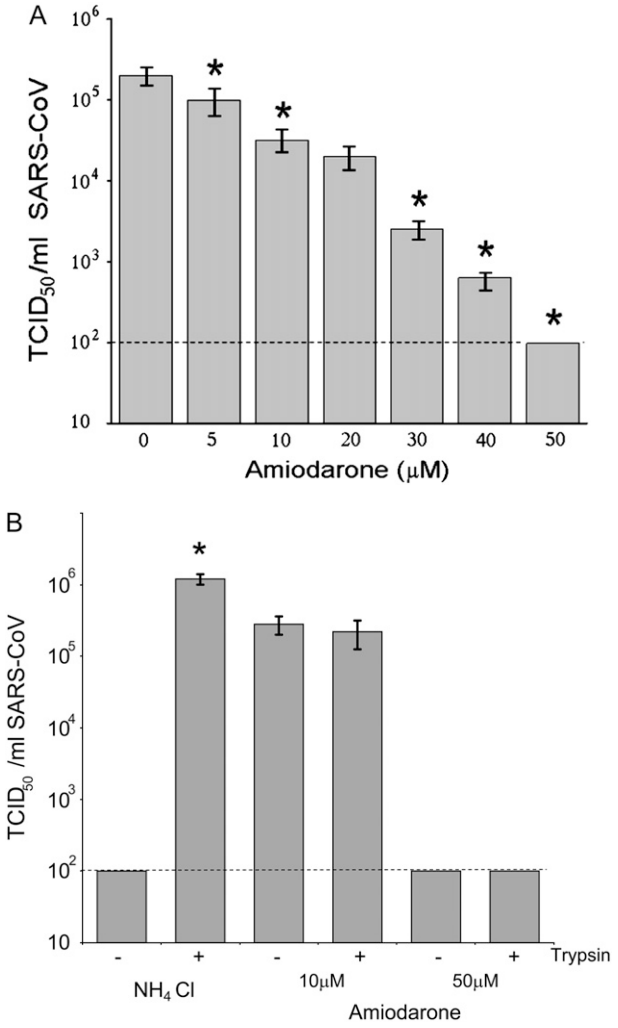

Figure 7. Effect of amiodarone on SARS-CoV infection. (*A*) Vero cells incubated for 2 hours with 0 to 50 μM amiodarone, exposed for 1 hour to SARS-CoV (1 m.o.i.) and incubated again with amiodarone for 24 hours. Virus concentration in the supernatant evaluated by titration in Vero cells. *Dotted line* = lower limit of detection. Representative of four experiments. *Significantly different from lower amiodarone concentration ($P < 0.05$). (*B*) Effect of NH_4Cl or amiodarone on the infectivity of trypsin-treated SARS coronavirus. Cells were incubated at 37°C for 2 hours with medium (control), 40 mM NH_4Cl, or amiodarone (10 or 50 μM). Afterwards cells were incubated for 1 hour at 4°C with SARS-CoV (1 m.o.i./cell) and then cell-bound virus was incubated for 5 minutes at 25°C with or without L-1-tosylamido-2-phenylethyl chloromethyl ketone-treated trypsin. Thereafter cells were incubated at 37°C for 24 hours with DMSO (controls), 40 mM NH_4Cl, or amiodarone (10 or 50 μM), and viral titer was determined in the supernatant. Representative of two experiments. *Significantly different from all others ($P < 0.05$). In both panels, values are means ± 95% confidence interval (Spearman-Karber).

that amiodarone perturbs selectively late compartment of the endocytic pthway (4, 7).

Biogenesis and proper functioning of late compartments of the endocytic pathway depend on a highly conserved set of protein (Hrs, ESCRT I-III, Alix) that assemble on the cytoplasmic side of early endosomes and make them mature into late endosomes/multivesicular bodies (27, 28). Recently it has been found that the suppression of hVps34, which converts phosphatidylinositol to phosphatidylinositol 3-phosphate (the docking site for SCRTIII), generates changes similar, although not identical, to those induced by amiodarone (29). These changes include sparing of early endosomes, formation of enlarged late endosomes, impaired endo-lysosomal proteolysis, and subtle disturbances in the maturation of cathepsin D (29). Thus, considering that ESCRT III is involved in the formation of multivesicular bodies (27, 28), it is tempting to speculate that amiodarone might act on a related target and that enlarged late endosomes might derive from the decreased formation of intralumenal vesicles.

We found previously that incubation of alveolar macrophages with 10.0 μM amiodarone decreases the size of the lysosomal compartment (4). This might explain the observation that, when presented to macrophages at low (0.2 μM) concentration, ^{125}I-amiodarone distributed mostly to lysosomes, whereas when presented at higher (10.2 μM) concentration, it distributed mostly to endosomes.

Shrinking of the lysosomal compartment could also explain the decreased uptake of Lysosensor by macrophages incubated with amiodarone.

Effects of Amiodarone on SARS-CoV Infection

Many enveloped viruses enter target cells by receptor-mediated endocytosis and their genetic material reaches the cytoplasm after fusion of viral and endosomal membranes. This process requires the rearrangement of a virus surface protein and the exposure of a hydrophobic domain, the fusion peptide (30). For many viruses such a rearrangement requires just the mildly acidic milieu of an endosomal compartment, but some viruses, like the Ebola virus and the SARS-CoV, also need the activity of an endosomal protease (14, 31). In the case of the SARS-CoV the protease needed for cell invasion is the endosomal protease cathepsin L. In fact, SARS-CoV infection can be blocked by inhibitors of V-ATPase, by lysosomotropic agents like ammonium chloride, and by inhibitors of cathepsin L (13).

Endosomal compartments and their proper functioning play an important role in the life cycle of the SARS-CoV; therefore, we thought that amiodarone, which inhibits endo-lysosomal hydrolysis and interferes with late compartments of the endocytic pathway, could interfere with virus entry into target cells. We found that amiodarone inhibits SARS-CoV infectivity and that inhibition appears to take place at a post-endosomal level, since amiodarone does not influence the surface density of ACE2, does not dissipate luminal acidity, does not impair synthesis and maturation of cathepsin L, and cannot be antagonized by the treatment of cell-bound virus with trypsin, which allows virus entry through the plasma membrane.

How amiodarone inhibits SARS-CoV amplification remains at present unclear; however, considering its effects on cell morphology (4, 7), it is tempting to speculate that it might interfere with steps of the virus life cycle involving cell membranes. For example, amiodarone could interfere with the assembly or function of virus-specific, flask-shaped cytoplasmic compartments bordered by a double membrane into which novel viral RNA is synthesized (32–34). Alternatively, amiodarone might interfere with the assembly of structural proteins and genomic RNA into new virions or might inhibit the release of progeny virus in the extracellular space, since the protein complexes necessary for the biogenesis of multivesicular bodies (the ESCRTs) also mediate virus budding (27). Furthermore, it is still possible that the antiviral effects of amiodarone could be occurring also in the endosomes.

Clearly, the evidence of an activity of amiodarone against the SARS-CoV is preliminary and its applicability in the clinic is

open to question, since the concentrations needed to obtain an antiviral effect *in vitro* are greater than serum levels found in patients treated for cardiac arrhythmias. We feel, however, that this subject deserves further scrutiny for several reasons. The first reason is that *in vivo* amiodarone is transformed into metabolites, which retain many of the activities displayed by the parent drug (7), and thus the antiviral activity of amiodarone would be much clarified by a test in an animal model of SARS, in the hope that amiodarone and its metabolites could cooperate against the virus. Another reason to study *in vivo* the antiviral activity of amiodarone stems from changes in virus tropism during the infection, since it has been suggested that at the start of the infection SARS-CoV may enter target cells through the endosomal pathway, while at later stages inflammation could liberate a variety of proteases that might induce virus entry through the plasma membrane, causing a further increase in the replication rate (15). We hypothesize that amiodarone could alleviate this mechanism of amplification, since *in vitro* its antiviral activity appears to be independent from the mechanism of virus entry into target cells. A further reason to perform protection studies in animals is that amiodarone could be tried in association with drugs that affect the virus life cycle by a different action mechanisms (16).

We conclude that amiodarone perturbs late compartments of the endocytic pathway and inhibits SARS coronavirus infection, acting after the delivery of the viral genome into the cytosol.

Conflict of Interest Statement: None of the authors has a financial relationship with a commercial entity that has an interest in the subject of this manuscript.

Acknowledgments: The authors thank professor Federico Rea for his help with the isolation of human alveolar macrophages.

References

1. Pollak PT, Bouillon T, Shafer SL. Population pharmacokinetics of long-term oral amiodarone therapy. *Clin Pharmacol Ther* 2000;67:642–652.
2. Van der Groot FG, Gruenberg J. Intraendosomal membrane traffic. *Trends Cell Biol* 2006;16:514–521.
3. Reasor MJ, Kacew S. Drug-induced phospholipidosis: are there functional consequences? *Exp Biol Med* 2001;226:825–830.
4. Baritussio A, Marzini S, Agostini M, Alberti A, Cimenti C, Bruttomesso D, Manzato E, Quaglino D, Pettenazzo A. Amiodarone inhibits lung degradation of SP-A and perturbs the distribution of lysosomal enzymes. *Am J Physiol Lung Cell Mol Physiol* 2001;281:L1189–L1199.
5. Mortuza GB, Neville WA, Delaney J, Waterfield CJ, Camilleri P. Characterization of a potential biomarker of phospholipidosis from amiodarone-treated rats. *Biochim Biophys Acta* 2003;1631:136–146.
6. Adams PC, Holt DW, Storey GC, Morley AR, Callaghan J, Campbell RW. Amiodarone and its desethyl metabolite: tissue distribution and morphological changes during long-term therapy. *Circulation* 1985;72: 1064–1068.
7. Quaglino D, Ha HR, Duner E, Bruttomesso D, Bigler L, Follath F, Realdi G, Pettenazzo A, Baritussio A. Effects of metabolites and analogs of amiodarone on alveolar macrophages: structure-activity relationship. *Am J Physiol Lung Cell Mol Physiol* 2004;287:L438–L447.
8. Stadler K, Masignani V, Eickmann M, Becker S, Abrignani S, Klenk H-D, Rappuoli R. SARS: beginning to understand a new virus. *Nat Rev Microbiol* 2003;1:209–218.
9. de Haan CAM, Rottier A, Hosting JM. The severe acute respiratory syndrome coronavirus: specific cell factors required for infection. *Cell Microbiol* 2006;8:1211–1218.
10. Li V, Moore MJ, Vasilieva N, Sui J, Wong SK, Berne MA, Somasundaran M, Sullivan JL, Luzuriaga K, Greenough TC, *et al.* Angiotensin-converting enzyme 2 is a functional receptor for the SARS coronavirus. *Nature* 2003;426:450–454.
11. Jeffers SA, Tusell SM, Gillim-Ross L, Hemmila EM, Achenbach JE, Babcock GJ, Thomas WD, Thackray LB, Young MD, Mason RJ, *et al.* CD209L (L-SIGN) is a receptor for severe acute respiratory syndrome coronavirus. *Proc Natl Acad Sci USA* 2004;101:15748–15753.
12. Simmons G, Reeves JD, Rennekamp AJ, Amberg SM, Piefer AJ, Bates P. Characterization of severe acute respiratory syndrome-associated coronavirus (SARS-CoV) spike glycoprotein-mediated viral entry. *Proc Natl Acad Sci USA* 2004;101:4240–4245.
13. Simmons G, Gosalia DN, Rennekamp AJ, Reeves JD, Diamond SL, Bates P. Inhibitors of cathepsin L prevent severe acute respiratory syndrome coronavirus entry. *Proc Natl Acad Sci USA* 2005;102: 11876–11881.
14. Huang I-C, Bosch BJ, Li F, Li W, Lee KH, Ghiran S, Vasilieva N, Dermody TS, Harrison SC, Dormitzer PR, *et al.* SARS coronavirus, but not coronavirus NL63 utilizes cathepsin L to infect ACE-2 expressing cells. *J Biol Chem* 2006;281:3198–3203.
15. Matsuyama S, Ujike M, Morikawa S, Tashiro M, Taguchi F. Protease-mediated enhancement of severe acute respiratory syndrome coronavirus infection. *Proc Natl Acad Sci USA* 2005;102:12543–12547.
16. Vincent MJ, Bergeron E, Benjannet S, Erickson BR, Rollin PE, Ksiazek TG, Seidah NG, Nichol ST. Chloroquine is a potent inhibitor of SARS coronavirus infection and spread. *Virol J* 2005;2:69–78.
17. Bellen JC, Penglis S, Tsopelas C. Radiolabeling and biodistribution of amiodarone and desethylamiodarone. *Nucl Med Biol* 1995;22:953–955.
18. Bergstrom CAS, Luthman K, Artursson P. Accuracy of calculated pH-dependent aqueous drug solubility. *Eur J Pharm Sci* 2004;22:387–398.
19. Ong S, Liu H, Qiu X, Bhat G, Pidgeon C. Membrane partition coefficients chromatographically measured using immobilized artificial membrane surfaces. *Anal Chem* 1995;67:755–762.
20. Kundra R, Kornfeld S. Wortmannin retards the movement of the mannose 6-phosphate/insulin-like factor II receptor and its ligand out of endosomes. *J Biol Chem* 1998;273:3848–3853.
21. Bradford MM. A rapid and sensitive method for the quantitation of microgram quantities of protein utilizing the principle of protein-dye binding. *Anal Biochem* 1976;72:248–254.
22. Baritussio AG, Magoon MW, Goerke J, Clements JA. Precursor-product relationship between rabbit type II cell lamellar body and alveolar surface active material. Surfactant turnover time. *Biochim Biophys Acta* 1981;666:382–393.
23. Kobayashi T, Beuchat M-H, Chevallier J, Makino A, Mayran N, Escola J-M, Lebrand C, Cosson P, Kobayashi T, Gruenberg J. Separation and characterization of late endosomal domains. *J Biol Chem* 2002; 277:32157–32164.
24. Eto K, Yamashita T, Hirose K, Tsubamoto Y, Ainscow EK, Rutter GA, Kimura S, Noda M, Iino M, Kadowaki T. Glucose metabolism and glutamase analog acutely alkalinize pH of insulin secretory vesicles of pancreatic β-cells. *Am J Physiol Endocrinol Metab* 2003;285:E262–E271.
25. Nepal RM, Mampe S, Shaffer B, Erickson A, Bryant P. Cathepsin L maturation and activity is impaired in macrophages harboring M. avium and M. tuberculosis. *Int Immunol* 2006;18:931–939.
26. Knapp PE, Swanson JA. Plasticity of the tubular lysosomal compartment in macrophages. *J Cell Sci* 1990;95:433–439.
27. Slagsvold T, Pattni K, Malerod L, Stenmark H. Endosomal and non-endosomal functions of ESCRT proteins. *Trends Cell Biol* 2006;16:317–326.
28. Williams RL, Urbè S. The emerging shape of the ESCRT machinery. *Nat Rev Mol Cell Biol* 2007;8:355–368.
29. Johnson EE, Overmeyer JH, Gunning WT, Maltese WA. Gene silencing reveals a specific function of hVps34 phosphatidylinositol 3-kinase in late versus early endosomes. *J Cell Sci* 2006;119:1219–1232.
30. Smith AE, Helenius A. How viruses enter animal cells. *Science* 2004;304: 237–242.
31. Chandran K, Sullivan NJ, Felbor U, Whelan SP, Cunningham JM. Endosomal proteolysis of Ebola virus glycoprotein is necessary for infection. *Science* 2005;308:1643–1645.
32. Snijder EJ, van der Meer Y, Zevenhoven-Dobbe J, Ondervater JJM, van der Meulen J, Koerten HK, Mommaas AM. Ultrastructure and origin of membrane vesicles associated with the severe acute respiratory syndrome coronavirus replication complex. *J Virol* 2006;80:5927–5940.
33. Stertz S, Reichelt M, Spiegel M, Kuri T, Martinez-Sobrido L, Garcia-Sastre A, Weber F, Kochs G. The intracellular sites of early replication and budding of SARS-coronavirus. *Virology* 2007;361:304–315.
34. Gosert R, Kanjanahaluethai A, Egger D, Bienz K, Baker SC. RNA replication of mouse hepatitis virus takes place at double-membrane vesicles. *J Virol* 2002;76:3697–3708.